The influence of particle breakage on the drained shear strength of calcareous sands

Houzhen Wei

Associate Professor, State Key Laboratory of Geomechanics and Geotechnical Engineering, Institute of Rock and Soil Mechanics, Chinese Academy of Sciences, Wuhan, 430071, China

E-mail: hzwei@whrsm.ac.cn

Coauthor: Xiaoxiao Li

Ph.D. Candidate, State Key Laboratory of Geomechanics and Geotechnical Engineering, Institute of Rock and Soil Mechanics, Chinese Academy of Sciences, Wuhan, 430071, China; University of Chinese Academy of Sciences, Beijing, 100049, China

E-mail: lixiaoxiao19@mails.ucas.ac.cn

Coauthor: Shuodong Zhang

Ph.D. Candidate, Department of Civil and Environmental Engineering, Brunel University London, London, UB8 3PH, United Kingdom

E-mail: shuodong.zhang@brunel.ac.uk

Corresponding author: Tao Zhao*

Lecturer, Department of Civil and Environmental Engineering, Brunel University London, London, UB8 3PH, United Kingdom

E-mail: tao.zhao@brunel.ac.uk

Coauthor: Mei Yin

Lecturer, Department of Civil and Environmental Engineering, Brunel University London, London, UB8 3PH, United Kingdom

E-mail: mei.yin@brunel.ac.uk

Coauthor: Qingshan Meng

Professor, State Key Laboratory of Geomechanics and Geotechnical Engineering, Institute of Rock and Soil Mechanics, Chinese Academy of Sciences, Wuhan, 430071, China

E-mail: qsmeng@whrsm.ac.cn

Abstract: The consolidated drained triaxial shear tests have been performed in this work to investigate the shearing behavior of calcareous sands sampled from the South China Sea, with the focus to analyze the influence of particle breakage on the materials shear strength. At approaching the failure limit state, the intense particle breakage and rearrangements prevented the shear stress from increasing further. Depending on the initial packing density, the loose sand sample exhibited the strain hardening response, while the dense sand sample exhibited the strain softening response with clear shear dilatancy after the peak shear strength has been reached. However, as the confining pressure increases, particle breakage occurred more thoroughly, and the sharpness of the peak stress disappeared gradually. For the series of tests, an upper limit of relative particle breakage existed, beyond which the confining pressure and relative density had little influence on the breakage of particles. The shear strength of calcareous sands was found to be determined by the combined effects of interparticle friction, sample dilatancy, and particle breakage. Under low confining pressures, the shear strength was mainly controlled by particle friction and sample dilatancy, while under high confining pressures, the effect of particle breakage was dominant. In this process, the volumetric strain evolved from dilatation to contraction and the sample dilatancy angle decreased gradually, as the particle shape transformed from highly angular to sub-rounded.

Keywords: Calcareous sands; triaxial shear test; particle breakage, shear strength, dilatancy

Declarations:

Funding: This research was supported by the Strategic Priority Research Program of the Chinese Academy of Sciences (grant XDA19060301 and grant XDA13010200), the National Natural Science Foundation of China (grant 41877260 and 41877267) and the open funding of the State Key Laboratory of Geomechanics and Geotechnical Engineering (No. Z019004). All these supports are acknowledged.

Conflicts of interest: The authors declare that they have no conflict of interest.

Ethics approval: Not applicable.

Consent to participate: Not applicable.

Consent for publication: The authors declare that this is an original paper which has neither previously been published, nor under consideration for publication anywhere else; that its publication has been approved by all co-authors. All the data is authentic and was developed by the authors.

Code availability: Not applicable.

Introduction

As a type of geotechnical materials, calcareous sands are deposits widely found in tropical marine environment. They are primarily composed of calcium carbonate or other insoluble carbonate materials. The sands have the characteristics of well-developed internal pore space, irregular shape, low strength, and high brittleness, which make their mechanical properties significantly different from the terrigenous counterpart soils (Xiao et al., 2019). These characteristics also lead to the unique property of particle breakage under even low stress and strain levels (Coop et al., 2004, Miao and Airey, 2013, Wei et al., 2018, Yu, 2017a).

The particle breakage has been widely recognized as the key factor influencing the overall mechanical behaviour of soil, including strength, deformation and permeability (David et al., 2011, Lade et al., 2010, Shahnazari and Rezvani, 2013, Wang et al., 2017, Xiao and Liu, 2017). During compression or shearing, particle breakage occurs when the loading stress exceeds the yielding stress of sands (Hyodo et al., 2002, Lade et al., 1996). This effect is particularly significant for uniformly graded samples (Bolton et al., 2008). The particle breakage induced by the shearing of aggregates is different from the crushing of rock mass, as the damage is concentrated mainly at particle edges and corners or particle surface abrasion due to the localized high contact stresses between particles. It is affected by many factors, such as the material property of constituent particles (e.g. strong minerals can hardly be crushed.) (Leleu and Valdes, 2007), particle size and shape (e.g. the probability of particle breakage increases with its size) (Norazirah et al., 2016, Xiao et al., 2020), particle size distribution (Gupta, 2017, Shen et al., 2019), relative density (Shahnazari and Rezvani, 2013), external loading stress (Parab et al., 2014), saturation condition (Alonso et al., 2016) and the loading duration (also known as creeping behaviour) (Fu et al., 2019).

In the literature, different types of laboratory experiments have been performed to investigate the influence of particle breakage on the mechanical responses of soil under drained condition, including the direct shear tests, triaxial shear tests and ring shear tests (Lade and Yamamuro, 1996, Luzzani and Coop, 2002, Wei et al., 2018). Detailed analyses revealed that the particle breakage can change the position of the critical-state locus in the plane of void ratio-mean effective stress (Xiao et al., 2016b), with the downward translation and an anticlockwise rotation (Yu, 2017b). The related studies also led to some well-developed constitutive models (Tengattini et al., 2016, Xiao et al., 2016a, Yao et al., 2008), such as the generalized plasticity model (Liu and Zou, 2013), the disturb state concept (Varadarajan et al., 2006) and the bounding surface model (Xiao and Liu, 2017). Hassanlourad et al. (2014) carried out consolidated and drained triaxial shear tests on four different types of sands to investigate their shear strengths via the energy approach. The results showed that the internal friction angle of carbonate sands has three contributing components, namely the particle surface friction, sample dilatancy and particle breakage. The effects of confining pressure and initial relative density of sample on each component have also been studied and explained. To investigate the influence of particle breakage on soil behaviour, Yu (2017a) performed a series of drained triaxial shear tests on precrushed coral sands and concluded that particle breakage can impair the dilatancy response of the sample, resulting in a more contractive behaviour. This process has a significant influence on the friction-dilatancy response of sands, such that both peak-state friction angle and dilatancy angle at the critical-state would decrease. The shearing process can also change the particle grading significantly as many fine particles are produced due to successive breakage of particles under the increased loading stress (McDowell and Bolton, 1998). This process would effectively change the granular packing state and material internal friction, leading to the dynamic variation of soil strength.

Though advancements exist, the evolutions of sample packing state, shear strength and volumetric strain induced by particle breakage during the triaxial shear tests are still not well-investigated. These limitations prompt a more systematic research as presented herein, with the purpose to explore the characteristics of particle breakage and its influence on the corresponding shear strength of soil.

Experimental procedure

Triaxial shear test of calcareous sands

In this research, a series of consolidated and drained triaxial shear tests have been conducted to study the strength and deformation characteristics of calcareous sands. Several tests on standard quartz sands were also performed for comparison purpose. The triaxial shear testing apparatus used in this study was the fully automatic triaxial instrument manufactured by Nanjing TKA Technology

Co., Ltd (TKA, 2020). It allowed the application of confining pressure up to 2 MPa and the vertical loading force up to 10 kN. The shear rate ranged from 0.0001 to 4.8 mm/min. The calcareous sands were sampled from a coral reef in one of the islands in South China Sea. The mineral compositions were mainly aragonite, dolomite and calcite. The chemical composition of calcareous sands was quantitatively analysed by the D8 ADVANCE X-ray diffractometer (Bruker, 2020). It consists of mainly $CaCO_3$ and $MgCO_3$ with the weight percentages of 81.08% and 11.55%, respectively. The particle size distributed in a narrow range of 1-2 mm, which was classified as poorly graded according to the unified soil classification system (ASTM, 2011). The use of poorly sorted sand sample would lead to higher particle breakages during compression when compare to the well-graded samples (Altuhafi and Coop, 2011). The basic physical parameters of the two types of sands are shown in Table 1, and the particle shapes are illustrated in Figure 1.

In this research, the relative density of calcareous sand samples ranged from 45% to 97%, while the confining pressure (σ_3) ranged from 100 kPa to 1200 kPa, respectively. To keep the uniformity, the triaxial specimens were prepared by slowly air pluviating calcareous sands in three layers into a 1 mm thick membrane tightly held in place. The specimen was tamped gently to reach the targeted height. The thick rubber membrane was used to avoid the potential piercing of angular particles under high confining pressures. The sample was then placed in a vacuum container with de-aired water under back-pressure for more than 2 hours to ensure that it was completely saturated. After that, the specimen was installed on the triaxial shear apparatus for isotropic consolidation until the sample volume remained unchanged. Then, the shearing loading was applied until the axial strain of the sample exceeded 20%. In this process, the drained testing condition was employed on the granular sample. Finally, the calcareous sand particles were dried for analysing the particle size grading.

Particle breakage analysis

The intensity of particle breakage can be quantified by the relative breakage (Br), which is related to the change of particle grading before and after the tests, as defined by Hardin (1985). The initial definition considers a grinding size limit of 0.074 mm, while Einav (2007) removed this size limitation and proposed a new concept of relative breakage index, Br_E. Another way of quantifying particle breakage considers explicitly the increase of particle surface area as coarse particles are gradually crushed into finer ones (Russell, 2011). Nevertheless, the calculation of this index usually requires a lot of assumptions.

For simplicity and consistency of the analysis, this research used the original definition of relative breakage by Hardin (1985). Specifically, at the end of the triaxial shear test, the middle one third of the sample was carefully retrieved from the container and the two ends of the sample were removed because the calcareous sands in these regions were barely crushed. The calcareous sands were completely dried and then sieved according to the laboratory testing specification. After sieving, the mass of calcareous sand particles in each size range were weighed and recorded. Based on the particle grading curves before and after the test, the relative particle breakage can be calculated.

Results

Stress-strain and volumetric strain behaviour

Figure 2 showed the evolutions of deviatoric stress (q) and volumetric strain (ε_v) with the axial strain (ε_a) of calcareous sand samples during the triaxial tests under different confining pressures (σ_3). In Figure 2(a), under relatively low confining pressures (e.g. σ_3 = 100 kPa), the calcareous sand sample of low relative density (Dr=45%) showed a strain-hardening behaviour throughout the test, with the peak strength occurring at a very large axial strain. As the relative density increases, the stress-strain curve evolved gradually from the strain hardening (ductile) to strain softening (brittle) behaviour. For dense samples, the peak shear strength occurred at a relatively small axial strain. After reaching the peak value, the higher the relative density, the faster the shear stress decreased. As the confining pressure increased, the sharpness of the stress-strain curve disappeared, and the soil exhibited only the strain hardening behaviour. Under very high confining pressures (e.g. σ_3 = 1200 kPa), the stress-strain curves of calcareous sands with different relative densities all showed similar evolution pattern of the strain hardening.

Figure 2 also illustrated the evolution of volumetric strain for calcareous sands under different confining pressures. Under low confining pressures (e.g. 100kPa), the dense calcareous sand samples (Dr > 65%) showed obvious shear-induced dilatancy, while the loose sample (Dr = 45%) only exhibited the contractive behaviour. The strain corresponding to the starting point of sample dilatation gradually decreased with the increase of sample relative density. At higher confining pressures, the volumetric strain showed purely the contractive behaviour, even though at p = 200 kPa, dense samples could still have the trend to dilate after some degree of contraction. For all the tests, the trend of sample dilation increased with its initial packing density. Under the extremely high confining pressure of 1200 kPa, the contractive volumetric strains of different samples showed very similar results and the peak values were not obvious within the current range of axial strain.

The mechanical behaviour of calcareous sands shown in Figure 2 were governed primarily by particle rearrangement and breakage during the shear deformation. Under low confining pressures, as quite a few particles were crushed, the initial relative density of the sample dominated the soil behaviour. The loose samples of low relative density needed to be compressed thoroughly before the occurrence of shear dilatation. Therefore, intense particle rearrangements existed within the sample, resulting in large axial strains before shear dilatation. As the relatively density increased, particles were packed increasingly closer to each other, resulting in a small volumetric contraction before the sample dilation. Thus, the axial strain corresponding to the start of shear dilatation was small. Under higher confining pressures, the compression of the solid skeleton was also accompanied by intense particle breakages. The crushed calcareous sands can produce a large number of fines which would fill up the voids between particles effectively, resulting in a much denser sample after the initial consolidation. This process could effectively consolidate the initial loose samples, transforming the packing state and mechanical behaviour similar to those of dense samples.

As a comparison, Figure 3 illustrated the mechanical behaviour of relatively dense quartz sand samples in consolidated drained triaxial tests under the confining pressures of 100 kPa and 1200 kPa, respectively. Similar strain softening and shear dilating behaviour of sands occurred under low confining pressure of 100 kPa. However, under the high confining pressure of 1200 kPa, the dense quartz sands can still exhibit clear strain softening behaviour, which is different from the response of calcareous sands. The difference was mainly due to the influence of particle breakage. For calcareous sands, particles could be crushed readily under high loading pressures, inducing additional volumetric contraction in addition to the normal consolidation. However, the particle breakage effect was not significant for quartz sands under high confining pressures due to the high material strength. For the dense quartz sand samples, the particle rearrangement (e.g. dislocation and tumbling) played a dominant role during the shearing process, resulting in obvious shear dilation. For the loose samples tested under high confining pressures, the skeleton of quartz sand particles was compressed gradually to a very dense state, exhibiting primarily the contractive behaviour.

Particle breakage during drained triaxial shear tests

The relationship between particle breakage and relative density

Figure 4(a) showed the gradation curves of calcareous sands after the triaxial shear tests under the confining pressure of 100 kPa. As shown in the figure, the percentage of fine particles increased with the relative density (Dr), indicating that particles can be readily crushed in densely packed state. In particular, the mass percentage of particles less than 1 mm (i.e. the finest particle size of the initial grading) increased from 23.1% at Dr=45% to 35.7% at Dr=93%. As a comparison, Figure 4(b) showed the gradation of calcareous sands under the high confining pressure of 1200 kPa. Under this loading condition, the particle breakage increased remarkably, that the mass percentage of particles finer than 1mm was about 51.1%. However, the difference of grading curves between tests on samples of various relative densities was very small, indicating that under high confining pressure, the relative density had a negligibly small influence on particle breakage.

The relative breakage of calcareous sands was calculated and presented in Figure 5, which showed a clear trend of the relative breakage increasing with the relative density of calcareous sands, following a linear relationship. The fitting function could be expressed as:

$$Br = a \cdot Dr + b \tag{1}$$

where a and b are the fitting parameters. Table 2 summarized the values of fitting parameters and their correlation coefficient R^2 for tests under different confining pressures. The slope a remained almost constant in the range of 0.043-0.057, except for the test under 1200 kPa as 0.012. The intercept b increased quickly with the confining pressure from 0.016 to 0.115, indicating that the confining pressure had a significant influence on particle breakage. It is worth noting that when the confining pressure was 1200 kPa, the variation of relative breakage with the increase of relative density was negligibly small. The results showed that after the confining pressure reaching a certain value, the influence of relative density on particle breakage would gradually disappear. Thus, an upper limit of particle breakage existed for these tests, such that beyond this value, the particle breakage could not increase any further. This result is similar to the research finding in Yamamuro and Lade (1996) for the shearing of quartz sands, with the upper limit of relative breakage of 0.35.

The relationship between particle breakage and confining pressure

Figure 6 (a) showed the gradation curves of the tests with various confining pressures for calcareous sands of the relative density Dr = 93%. The curves shifted gradually upwards as the confining pressure increased, indicating that more fine particles had been produced during the triaxial shearing process under high confining pressures. For all tests, the mass percentage of particles finer than 0.1 mm was very low because fine particles can effectively resist the external loading. Figure 6 (b) illustrated that for the loose (Dr = 45%) and dense (Dr = 93%) samples, the relative breakage of calcareous sands increased with the confining pressure following power law relationships. The dense samples generally had higher relative breakages than the looser ones. When the confining pressure reached 1200 kPa, the relative breakage was very close for the loose and dense samples, indicating that under the extremely high confining pressures, the particle breakage intensity tended to converge, which was independent of the initial granular packing state.

Influence of particle breakage on drained shear strength

As discussed in Alshibli and Cil (2018), the shear strength of uncemented granular materials (e.g. sands) has three major contributors, namely the sliding friction by surface roughness, sample dilatancy by particle rearrangement and interlocking, and particle breakage. The sliding friction is the intrinsic property of material surface roughness, which may vary slightly when particle breakage and surface abrasion occur. Thus, the variation of internal friction angle is influenced mainly by the combined effect of shear dilatancy and particle breakage. The proportion of the two friction contributors depends mainly on the testing conditions. For dense sands under low confining pressures, the change of internal friction angle depends mainly on shear dilatancy, while the effect of particle breakage is not significant. However, under high confining pressures, the sample dilatancy is negligible and the change of internal friction angle is influenced mainly by particle breakage. This indicates that when the stress level reached the threshold value of particle breakage, the characteristics of sand dilatation would be weakened or even diminished.

Peak friction angle, φ_p

According to previous analyses, when the confining pressure was higher than 200 kPa, a large number of calcareous sands could be crushed with significantly reduced particle interlocking intensity, which led the sample dilatancy to diminish gradually. Under such an experimental condition ($\sigma_3 > 200$ kPa), the sands showed a strain hardening behaviour with the peak stress occurring at failure and the peak friction angle (φ_p) was equal to the final critical state or residual friction angle (φ_{cs}). Figure 7 showed that in the experiments, the peak friction angle φ_p of the loose and dense calcareous sand samples decreased with the increase of confining pressures. The calcareous sands exhibited a high peak friction angle (35° - 42°) under low confining pressures (e.g. 200 kPa), while it was only around 20°-25° at high confining pressures (e.g. 1200 kPa). Throughout the test, regardless of the magnitude of the confining pressure, the test results for the dense specimens were always higher than the looser ones by about 2-7°.

According to the Mohr-Coulomb theory, the internal friction angle (φ) of the non-cohesive and non-crushable soil is always a constant value, which is only affected by the material property and the initial packing density of the sample. By ignoring the intermediate principal stress, the peak friction angle can be calculated by the following equation (Hassanlourad et al., 2014):

$$\varphi_p = \arcsin\frac{\left(\sigma_1' - \sigma_3'\right)_f}{\left(\sigma_1' + \sigma_3'\right)_f} = \arcsin\frac{\left(\sigma_1'/\sigma_3'\right)_f - 1}{\left(\sigma_1'/\sigma_3'\right)_f + 1} \tag{2}$$

In Eq.(2), the ratio of principal stresses $\left(\sigma_1'/\sigma_3'\right)_f$ at failure, namely $\left(\sigma_1'/\sigma_3'\right)_{\max}$ should be a constant value. Thus, the peak friction angle φ_p must be a constant for non-crushable materials. However, for calcareous sand, since particle breakage becomes increasingly significant with the increase of confining pressure, it would result in the decrease of $\left(\sigma_1'/\sigma_3'\right)_{\max}$ and thus the decrease of φ_p. This is illustrated in Figure 8 that the peak friction angle of the calcareous sands decreased with the relative breakage, following a power law relationship. As expected, at the same particle breakage level, the peak friction angle increased with the initial relative density of the sample.

Dilatancy angle, φ_{cv}

The dilatancy angle was reported to be related to the difference between the peak (φ_p) and critical state (φ_{cs}) friction angle (Bolton, 1986) by the following equation as,

$$\varphi_{cv} = 2\left(\varphi_p - \varphi_{cs}\right) \tag{3}$$

Considering the variations of relative density (Dr) and mean effective stress at failure $\left(p = \left(\sigma_1 + 2\sigma_3\right)/3\right)$, $\varphi_p - \varphi_{cs}$ can also be expressed as,

in Bolton (1986):

$$\varphi_p - \varphi_{cs} = 3\left(Dr\left(10 - \ln p\right) - 1\right) \tag{4}$$

and in Hasan and Alshibli (2010):

$$\varphi_p - \varphi_{cs} = 16\frac{Dr^{0.9}}{p^{0.1}} \tag{5}$$

According to Figure 2 and Figure 3, only under relatively low confining pressures (e.g. 100 kPa), the calcareous sands with the initial relative densities ranging from 65% to 93% could exhibit clear shear dilation responses. The corresponding dilatancy angles calculated by Eq. (3) were reported in Figure 9 as in the range of 14° to 19°. In general, the dilatancy angle increased with the initial relative density of the sample. Whereas, it increased very little when the relative density was higher than 80%, partly because of the particle breakage during the triaxial shearing which significantly reduced the sample dilation. The predictions by Eq.(4) was only slightly lower than the experimental results, even though it was reported not suitable for highly angular particles, such as calcareous sands (Hasan and Alshibli, 2010). The agreement of experimental data with the prediction by Eq.(4) could be explained by the change of particle shape from highly angular to sub-rounded due to particle breakage and abrasion during the test. The results given by Eq.(5) could overestimate the dilatancy angle of the dense sample as the effect of particle breakage had not been included in the model.

Discussion

In this study, the stress-strain and volumetric strain-axial strain relationships of calcareous sands evolved gradually from the strain softening to hardening behaviour when the confining pressure increased. In this process, the development of shear stress along the shear plane played a key role. In general, the external loading acting on the sample is resisted by the interparticle friction (shear stress, τ) and the normal stress (normal stress, σ) at the contact points. When the friction between particles are fully utilized, namely the friction is equal to the sand strength, $\tau = \sigma \tan\phi$, the shear stress cannot increase any further even though the normal stress continued to increase. Therefore, without considering particle breakage, the stress-strain relationship of calcareous sands is determined fundamentally by the interparticle frictions, including the contributions of sliding friction, rolling friction and particle interlocking. However, as a type of brittle materials, calcareous sands can be readily crushed under even low normal and shear loadings at contacts. Considering this, the stress state and deformation should be determined by the lower value of stress required to mobilize either the sliding or particle breakage process (see the illustrations in Figure 10). If the loading stress is high enough to initiate the particle breakage, but low to mobilize the sliding, the particle breakage would occur (Figure 10 (b)), while on the contrary, the shear stress would increase until the shear strength is reached to initiate sliding (Figure 10 (c)). Therefore, when particle breakage exists, the material shear strength should be controlled by the combined contributions of particle friction and breakage. The friction will increase the shear stress to the peak value and produce the strain-softening response, while particle breakage will reduce the shear stress and keep it in an intermediate value, producing the strain-hardening response. This process also determines the value of dilatancy angle of the sample.

For experiments conducted in this research, the low confining pressure was not effective in crushing the particles. Thus, the sample exhibited only the strain-softening behaviour with clear peak shear stress (i.e. the peak shear strength). After reaching the peak value, the particle sliding occurred, creating a layer of shear band within the sample which quickly reduced the shear stress until the stable residual shear strength was reached. The dense sample had a very small deformation before reaching the peak shear strength. Thus, the corresponding axial strain of the sample at the peak shear strength decreased with the relative density. On the other hand, under high confining pressures, particle breakage occurred more thoroughly for calcareous sands of various relative densities. As a result, the void spaces between particles were filled up with the fines and the peak shear strength of strain softening behaviour cannot be reached. Instead, the granular sample would exhibit the strain-hardening behaviour with the residual shear strength.

Conclusions

In this paper, the mechanical behavior of calcareous sands of different relative densities tested under different confining pressures have been investigated via the consolidated and drained triaxial shear tests. By comparing with the quartz sand, the particle breakage and its influence on the strength of calcareous sands have been explored. The major findings are summarized as:

1. At approaching the critical state, intense particle sliding, rolling and breakage occured, which prevented the loading stress from increasing further. Thus, the shear strength of calcareous sands was relatively low when compared to the quartz sands. Under the given experimental conditions, the sample deformation was mainly the particle sliding and rolling at low confining pressures,

resulting in the strain softening behavior. The strength of calcareous sands was the combined result of the friction by surface roughness, sample dilatancy by particle rearrangement and interlocking, and particle breakage. At high confining pressures, particle breakage occurred more thoroughly during the shearing process and the strain hardening behavior was obtained.

2. The volumetric deformation of the sample developed gradually from dilation to contraction. In this process, the degree of sample contraction increased with the intensity of particle breakage. As the sample dilatancy diminished, the particle interlocking effect was significantly weakened, leading to the decrease of the peak friction angle and thus the shear strength. Thus, the strength of calcareous sands was mainly affected by the combined effects of particle sliding and particle breakage.
3. The effect of relative density on particle breakage was less significant than the confining pressure. With the increase of confining pressure, the rate of particle breakage gradually decreased until it reached an upper limit. At this point, the confining pressure and relative density had little influence on particle breakage.

According to this research, the strength of calcareous sands is dependent on the stress level, which is effectively a state variable. Therefore, when calcareous sands as construction materials, it is necessary to consider the in-situ stress condition and particle breakage during the construction and carry out relevant tests to obtain reliable material strength parameters.

Data availability

All data generated during the study are available from the corresponding author by request.

Acknowledgements

This research was supported by the Strategic Priority Research Program of the Chinese Academy of Sciences (grant XDA19060301 and grant XDA13010200), the National Natural Science Foundation of China (grant 41877260 and 41877267) and the open funding of the State Key Laboratory of Geomechanics and Geotechnical Engineering (No. Z019004). All these supports are acknowledged.

References

Alonso, E. E., Romero, E. E., and Ortega, E. (2016). "Yielding of rockfill in relative humidity-controlled triaxial experiments." *Acta Geotechnica*, 11(3), 455-477.

Alshibli, K. A., and Cil, M. B. (2018). "Influence of Particle Morphology on the Friction and Dilatancy of Sand." *J. Geotech. Geoenviron.*, 144(3), 04017118.

Altuhafi, F. N., and Coop, M. R. (2011). "Changes to particle characteristics associated with the compression of sands." *Géotechnique*, 61(6), 459-471.

ASTM (2011). *ASTM D2487-11: Standard Practice for Classification of Soils for Engineering Purposes (Unified Soil Classification System)*, ASTM International, West Conshohocken, PA, USA.

Bolton, M. D. (1986). "The strength and dilatancy of sands." *Géotechnique*, 36(1), 65-78.

Bolton, M. D., Nakata, Y., and Cheng, Y. P. (2008). "Micro- and macro-mechanical behaviour of DEM crushable materials." *Géotechnique*, 58(6), 471-480.

Bruker (2020). "D8 ADVANCE Structure Analysis - X-ray Diffraction." *https://www.bruker.com/*.

Coop, M. R., Sorensen, K. K., Freitas, T. B., and Georgoutsos, G. (2004). "Particle breakage during shearing of a carbonate sand." *Géotechnique*, 54(3), 157-163.

David, W. A., John, P. C., and Martin, D. L. (2011). "Sydney Soil Model. II: Experimental Validation." *Int. J. Geomech.*, 11(3), 225-238.

Einav, I. (2007). "Breakage mechanics—Part I: Theory." *J. Mech. Phys. Solids*, 55(6), 1274-1297.

Fu, Z., Chen, S., Zhong, Q., and Zhang, Y. (2019). "Modeling interaction between loading-induced and creep strains of rockfill materials using a hardening elastoplastic constitutive model." *Canadian Geotechnical Journal*, 56(10), 1380-1394.

Gupta, V. (2017). "Effect of size distribution of the particulate material on the specific breakage rate of particles in dry ball milling." *Powder Technology*, 305, 714-722.

Hardin, B. O. (1985). "Crushing of soil particles." *Journal of geotechnical engineering*, 111(10), 1177-1192.

Hasan, A., and Alshibli, K. A. (2010). "Discrete Element Modeling of Strength Properties of Johnson Space Center (JSC-1A) Lunar Regolith Simulant." *Journal of Aerospace Engineering*, 23(3), 157-165.

Hassanlourad, M., Salehzadeh, H., and Shahnazari, H. (2014). "Drained shear strength of carbonate sands based on energy approach." *International Journal of Geotechnical Engineering*, 8(1), 1-9.

Hyodo, M., Hyde, A. F. L., Aramaki, N., and Nakata, Y. (2002). "Undrained monotonic and cyclic shear behaviour of sand under low and high confining stresses." *Soils and Foundations*, 42(3), 63-76.

Lade, P., Yamamuro, J., and Bopp, P. (1996). "Significance of Particle Crushing in Granular Materials." *Journal of Geotechnical Engineering*, 122(4), 309-316.

Lade, P. V., Nam, J., and Liggio Jr, C. D. (2010). "Effects of particle crushing in stress drop-relaxation experiments on crushed coral sand." *Journal of geotechnical and geoenvironmental engineering*, 136(3), 500-509.

Lade, P. V., and Yamamuro, J. A. (1996). "Undrained Sand Behavior in Axisymmetric Tests at High Pressures." *Journal of Geotechnical Engineering*, 122(2), 120-129.

Leleu, S., and Valdes, J. (2007). "Experimental study of the influence of mineral composition on sand crushing." *Géotechnique*, 57(3), 313-317.

Liu, H., and Zou, D. (2013). "Associated Generalized Plasticity Framework for Modeling Gravelly Soils Considering Particle Breakage." *Journal of Engineering Mechanics*, 139(5), 606-615.

Luzzani, L., and Coop, M. R. (2002). "On the relationship between particle breakage and the critical state of sands." *Soils and Foundations*, 42(2), 71-82.

McDowell, G. R., and Bolton, M. D. (1998). "On the micro-mechanics of crushable aggregates." *Géotechnique*, 48(5), 667-679.

Miao, G., and Airey, D. (2013). "Breakage and ultimate states for a carbonate sand." *Géotechnique*, 63(14), 1221-1229.

Norazirah, A., Fuad, S., and Hazizan, M. (2016). "The effect of size and shape on breakage characteristic of mineral." *Procedia Chemistry*, 19, 702-708.

Parab, N. D., Claus, B., Hudspeth, M. C., Black, J. T., Mondal, A., Sun, J., Fezzaa, K., Xiao, X., Luo, S., and Chen, W. (2014). "Experimental assessment of fracture of individual sand particles at different loading rates." *International Journal of Impact Engineering*, 68, 8-14.

Russell, A. R. (2011). "A compression line for soils with evolving particle and pore size distributions due to particle crushing." *Géotechnique Letters*, 1(1), 5-9.

Shahnazari, H., and Rezvani, R. (2013). "Effective parameters for the particle breakage of calcareous sands: An experimental study." *Engineering Geology*, 159, 98-105.

Shen, C., Liu, S., Wang, L., and Wang, Y. (2019). "Micromechanical modeling of particle breakage of granular materials in the framework of thermomechanics." *Acta Geotechnica*, 14(4), 939-954.

Tengattini, A., Das, A., and Einav, I. (2016). "A constitutive modelling framework predicting critical state in sand undergoing crushing and dilation." *Géotechnique*, 66(9), 695-710.

TKA (2020). "Fully automatic triaxial instrument." http://en.tkatest.com/product/176.html.

Varadarajan, A., Sharma, K. G., Abbas, S. M., and Dhawan, A. K. (2006). "Constitutive Model for Rockfill Materials and Determination of Material Constants." *Int. J. Geomech.*, 6(4), 226-237.

Wang, X.-Z., Wang, X., Jin, Z.-C., Meng, Q.-S., Zhu, C.-Q., and Wang, R. (2017). "Shear characteristics of calcareous gravelly soil." *Bulletin of Engineering Geology and the Environment*, 76(2), 561-573.

Wei, H., Zhao, T., He, J., Meng, Q., and Wang, X. (2018). "Evolution of Particle Breakage for Calcareous Sands during Ring Shear Tests." *Int. J. Geomech.*, 18(2), 04017153.

Xiao, Y., and Liu, H. (2017). "Elastoplastic Constitutive Model for Rockfill Materials Considering Particle Breakage." *Int. J. Geomech.*, 17(1), 04016041

Xiao, Y., Liu, H., Desai, C. S., Sun, Y., and Liu, H. (2016a). "Effect of Intermediate Principal-Stress Ratio on Particle Breakage of Rockfill Material." *J. Geotech. Geoenviron.*, 142(4), 06015017.

Xiao, Y., Liu, H., Ding, X., Chen, Y., Jiang, J., and Zhang, W. (2016b). "Influence of Particle Breakage on Critical State Line of Rockfill Material." *Int. J. Geomech.*, 16(1), 04015031.

Xiao, Y., Long, L., Evans, T. M., Zhou, H., Liu, H., and Stuedlein, A. W. (2019). "Effect of Particle Shape on Stress-Dilatancy Responses of Medium-Dense Sands." *J. Geotech. Geoenviron.*, 145(2), 04018105.

Xiao, Y., Meng, M., Daouadjie, A., Chen, Q., Wu, Z., and Jiang, X. (2020). "Effects of particle size on crushing and deformation behaviors of rockfill materials." *Geoscience Frontiers*, 11(2), 375-388.

Yamamuro, J. A., and Lade, P. V. (1996). "Drained sand behavior in axisymmetric tests at high pressures." *Journal of Geotechnical Engineering*, 122(2), 109-119.

Yao, Y.-P., Yamamoto, H., and Wang, N.-D. (2008). "Constitutive model considering sand crushing." *Soils and Foundations*, 48(4), 603-608.

Yu, F. W. (2017a). "Particle Breakage and the Drained Shear Behavior of Sands." *Int. J. Geomech.*, 17(8), 04017041.

Yu, F. W. (2017b). "Particle breakage and the critical state of sands." *Géotechnique*, 67(8), 713-719.

Table 1. The basic physical parameters of the samples.

Sand type	**Minimal void ratio, e_{min}**	**Maximal void ratio, e_{max}**	**Specific gravity**	**Diameter** (mm)
Calcareous sands	0.62	1.44	2.65	1.0-2.0
Quartz sands	1.27	1.87	2.79	1.0-2.0

Table 2. Fitting values of parameters in Eq. (1).

Confining Pressure/kPa	***a***	***b***	**R^2**
100	0.043	0.016	0.591
200	0.048	0.035	0.836
400	0.057	0.045	0.782
800	0.045	0.079	0.870
1200	0.012	0.115	0.748

Figure captions

Figure 1. The photos of two types of sands: a) Calcareous sands and b) Quartz sands.

Figure 2. Evolutions of deviatoric stress and volumetric strain of calcareous sand sample during the consolidated drained triaxial shear tests under various confining pressures: a)100 kPa, b) 200 kPa, c) 400 kPa, d)1200 kPa.

Figure 3. Evolutions of deviatoric stress and volumetric strain for quartz sands during the drained triaxial tests under the confining pressures of a)100kPa and b)1200kPa.

Figure 4. The gradation curves of calcareous sands with different relative densities after the drained triaxial shear tests under the confining pressure of a)100 kPa and b)1200 kPa.

Figure 5. The relationship between relative breakage (Br) and relative density (Dr).

Figure 6. a) The gradation curves of calcareous sands after the drained triaxial shear tests under different confining pressures with the relative density Dr = 93%; b) The relationship between particle relative breakage (Br) and confining pressure (p).

Figure 7. The relationship between the peak friction angle and effective confining pressure for the loose (Dr=45%) and dense (Dr=93%) calcareous sand samples.

Figure 8. The relationship between peak friction angle $\left(\varphi'_{\max}\right)$ and relative breakage (Br) for the loose (Dr=45%) and dense (Dr=93%) calcareous sand samples.

Figure 9. The relationship between dilatancy angle (φ_{cv}) and relative density (*Dr*). The confining pressure in the triaxial shear test was 100 kPa.

Figure 10. Schematic view of triaxial shear tests: (a) loading of the tests. The blue dashed region represents the shear band; (b) illustration of particle breakage under high confining pressure; (c) illustration of particle rearrangement (sliding and rolling) for tests under low confining pressures.

Figure 11. The photos of two types of sands: a) Calcareous sands and b) Quartz sands.

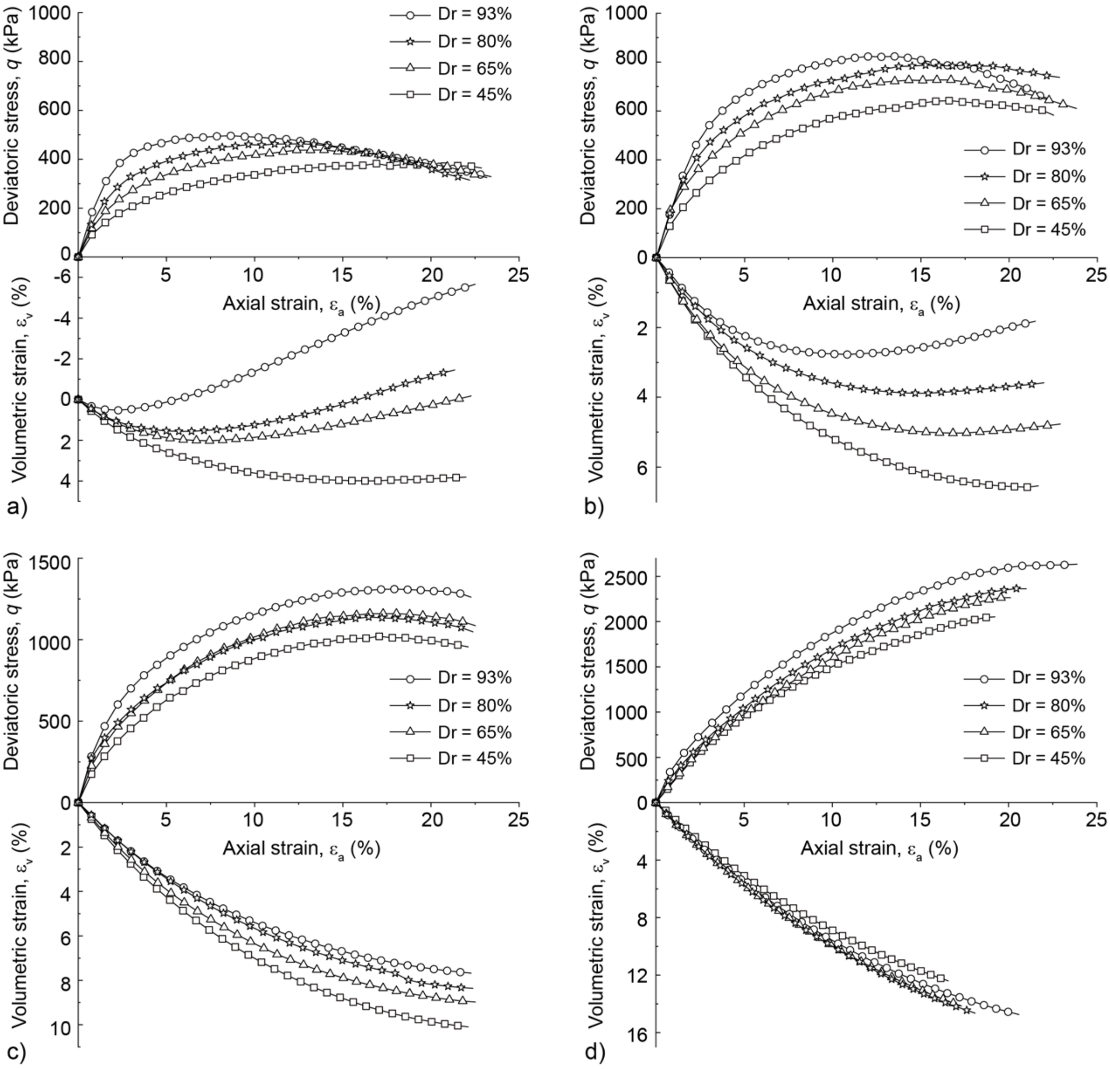

Figure 12. Evolutions of deviatoric stress and volumetric strain of calcareous sand sample during the consolidated drained triaxial shear tests under various confining pressures: a)100 kPa, b) 200 kPa, c) 400 kPa, d)1200 kPa.

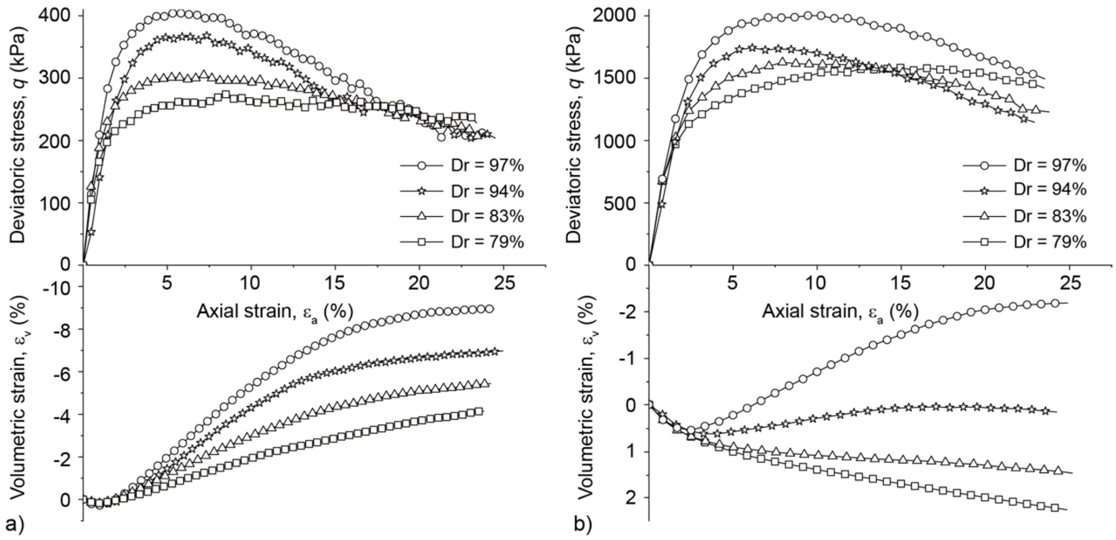

Figure 13. Evolutions of deviatoric stress and volumetric strain for quartz sands during the drained triaxial tests under the confining pressures of a)100kPa and b)1200kPa.

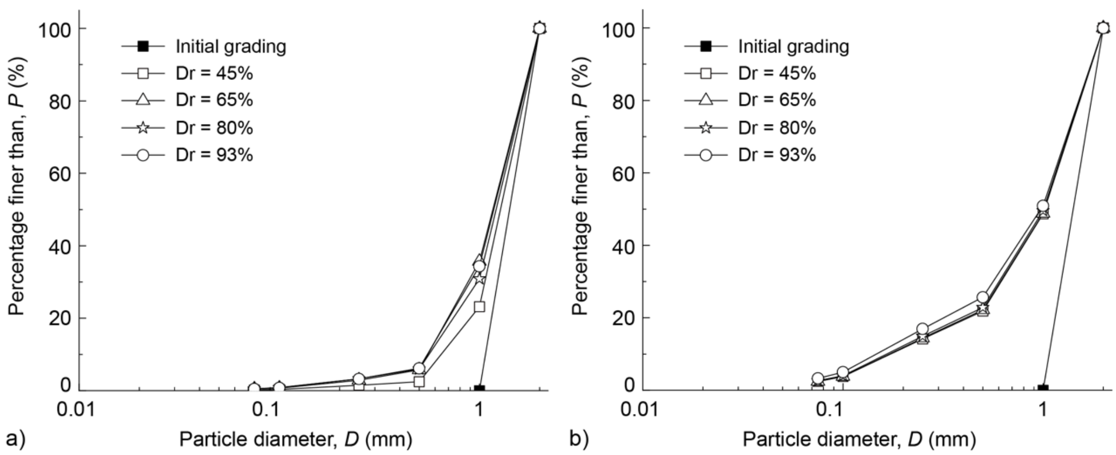

Figure 14. The gradation curves of calcareous sands with different relative densities after the drained triaxial shear tests under the confining pressure of a)100 kPa and b)1200 kPa.

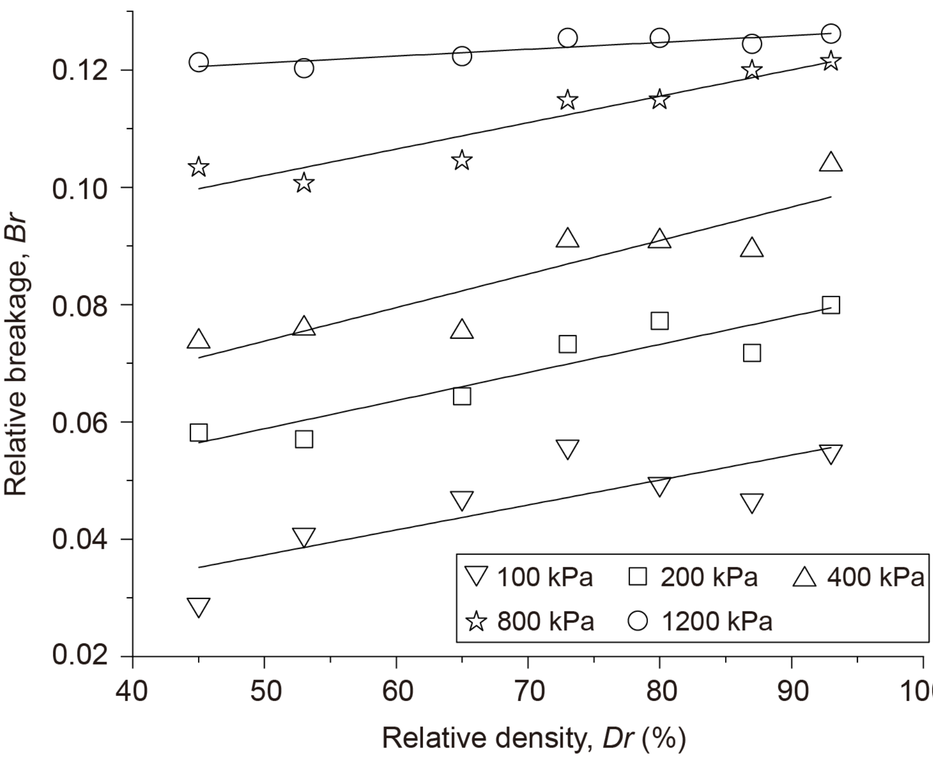

Figure 15. The relationship between relative breakage (Br) and relative density (Dr).

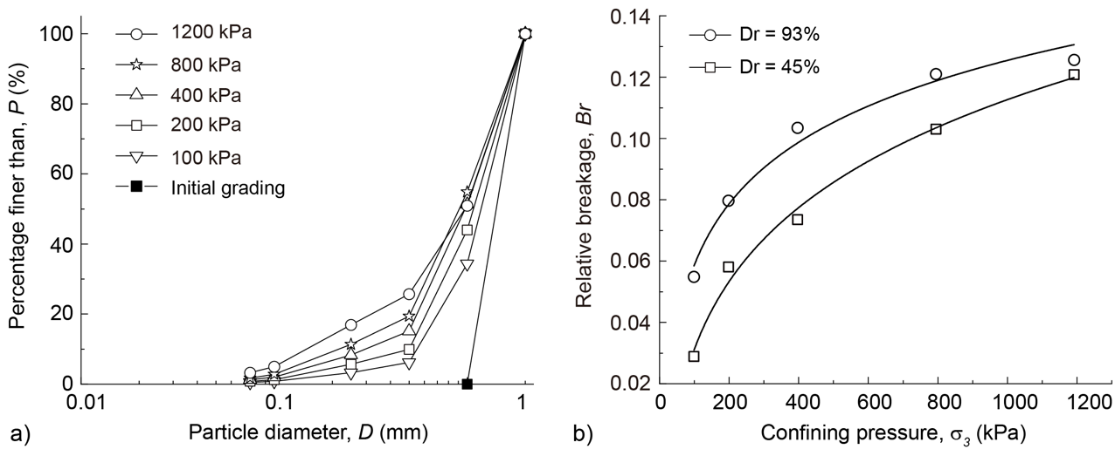

Figure 16. a) The gradation curves of calcareous sands after the drained triaxial shear tests under different confining pressures with the relative density Dr = 93%; b) The relationship between particle relative breakage (Br) and confining pressure (p).

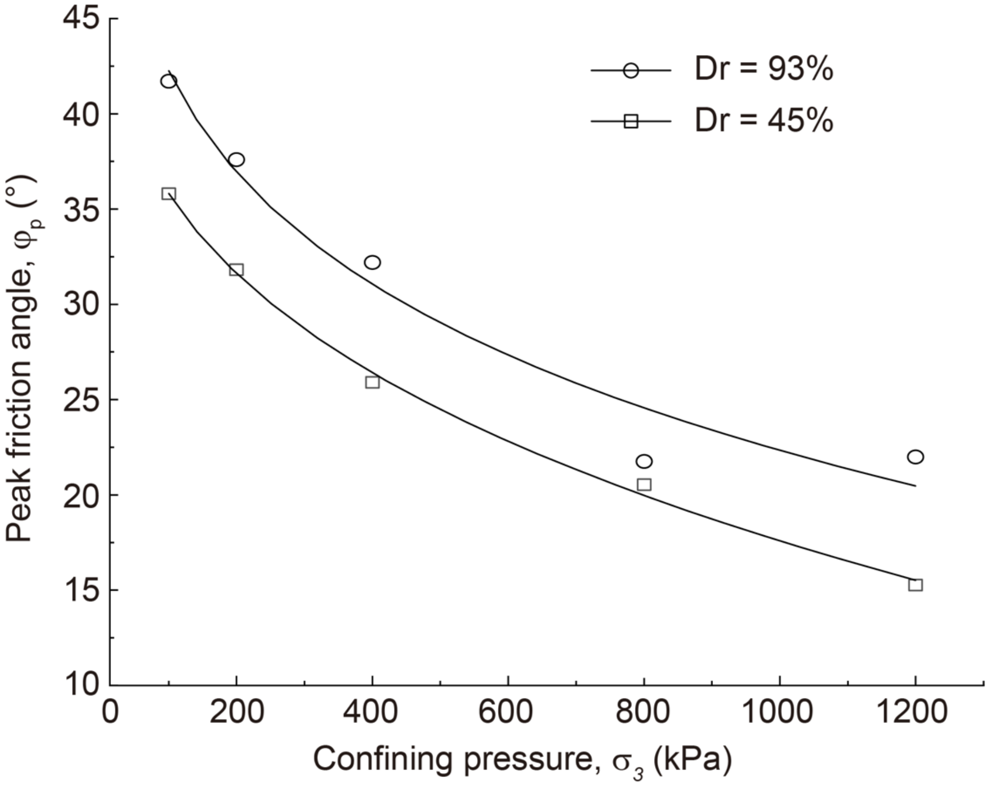

Figure 17. The relationship between the peak friction angle and effective confining pressure for the loose (Dr=45%) and dense (Dr=93%) calcareous sand samples.

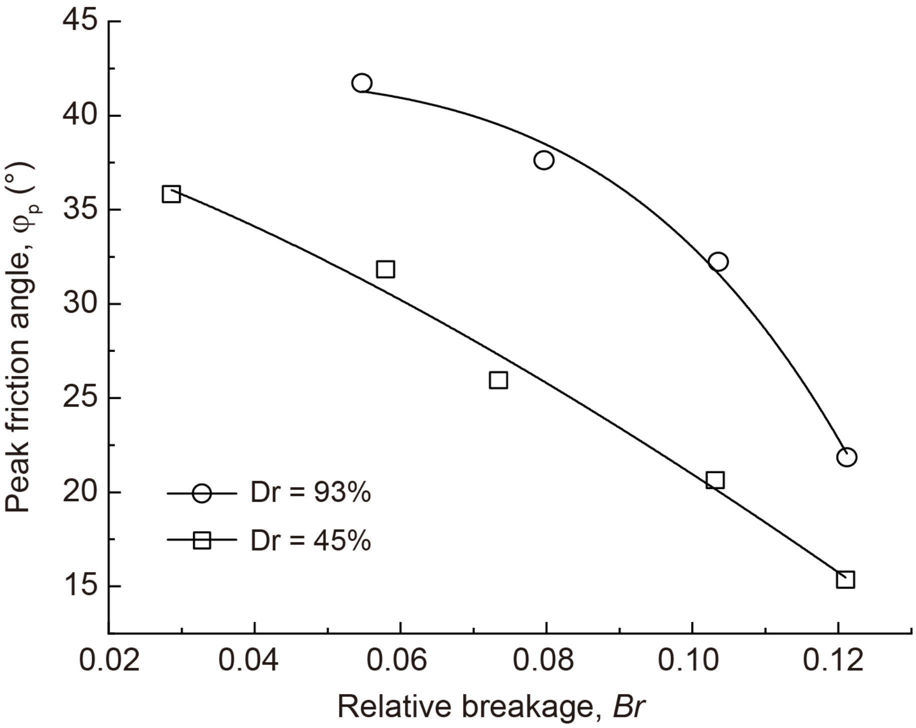

Figure 18. The relationship between peak friction angle (φ'_{max}) and relative breakage (Br) for the loose (Dr=45%) and dense (Dr=93%) calcareous sand samples.

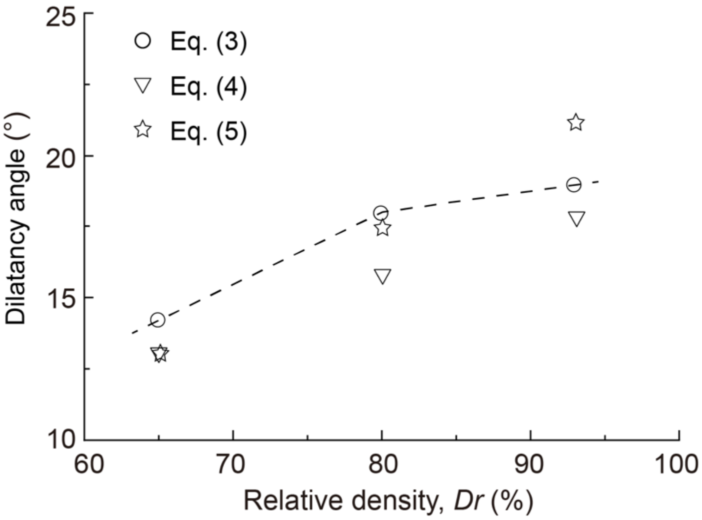

Figure 19. The relationship between dilatancy angle (φ_{cv}) and relative density (*Dr*). The confining pressure in the triaxial shear test was 100 kPa.

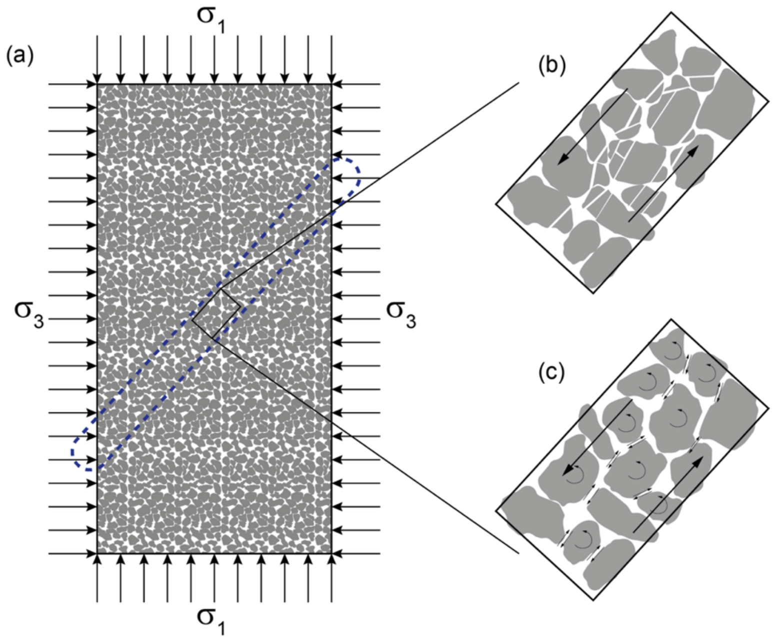

Figure 20. Schematic view of triaxial shear tests: (a) loading of the tests. The blue dashed region represents the shear band; (b) illustration of particle breakage under high confining pressure; (c) illustration of particle rearrangement (sliding and rolling) for tests under low confining pressure.

Table 3. The basic physical parameters of the samples.

Sand type	Minimal void ratio, e_{min}	Maximal void ratio, e_{max}	Specific gravity	Diameter (mm)
Calcareous sands	0.62	1.44	2.65	1.0-2.0
Quartz sands	1.27	1.87	2.79	1.0-2.0

Table 4. Fitting values of parameters in Eq. (1).

Confining Pressure/kPa	*a*	*b*	R^2
100	0.043	0.016	0.591
200	0.048	0.035	0.836
400	0.057	0.045	0.782
800	0.045	0.079	0.870
1200	0.012	0.115	0.748